Available online at www.sciencedirect.com
SCIENCE DIRECT®
Journal of Nuclear Materials 336 (2005) 163–172
journal of nuclear materials
www.elsevier.com/locate/jnucmat

Kinetics of the actinides–lanthanides separation: mass transfer between molten fluorides and liquid metal at high temperatures

Florent Lemort [a,*], Roger Boen [a], Michel Allibert [b], Damien Perrier [c], Yves Fautrelle [c], Jacqueline Etay [c]

[a] Commissariat à l'Énergie Atomique, CEA-Marcoule, BP 171, 30207 Bagnols-sur-Cèze cedex, France
[b] LTPCM-ENSEEG, BP 75, 38402 Saint Martin d'Hères, France
[c] CNRS-EPM-Madylam – ENSHMG BP 95 – 38402 St Martin d'Hères cedex, France

Received 8 June 2004; accepted 17 September 2004

Abstract

Experimental studies on the extraction of actinides and other elements from a fluorinated salt into a liquid metal phase containing a reducing agent such as magnesium or aluminium have been performed using two different systems. The rate of transfer is very rapid and could, depending on the way stirring is carried out, vary with the stirring rate. Three different types of stirring have been tested and observations are explained both in terms of hydrodynamics and chemistry. The role of interfacial agitation is discussed and the assumption that the limiting factor is related to the chemical reaction and not mass transfer is confirmed by a measured activation energy of $180\,\mathrm{kJ\,mol^{-1}}$. Thermal effects are observed with different magnitudes depending on the reduced species. Chemical control of the kinetics combined with thermal effects account for the rapid transfer. These results can be used to develop a high-temperature process for separating actinides and lanthanides. More work is required to determine the reaction mechanisms, which may not be limited to the interface.

1. Introduction

Studies of high-temperature material transfer kinetics involving chemical reactions in two-phase liquid systems have shown that they are generally controlled by diffusion in the transfer boundary layer [1]. Stirring of the system is thus a major factor in controlling the reaction rate. This is the case, for example, in metallurgical applications.

The present paper focuses on the kinetics of the transfer of an element M from a fluorinated phase into a metallic phase. MF_x is reduced by a reducing agent R. This process is shown in Fig. 1 and corresponds to the oxygen–reduction reaction, expressed for one mole of F_2 as

$$\frac{2}{x}\mathrm{MF}_x + \frac{2}{y}\mathrm{R} \leftrightarrow \frac{2}{x}\mathrm{M} + \frac{2}{y}\mathrm{RF}_y. \quad (1)$$

The transfer coefficient k_j is determined by measuring the concentration of R or M in the saline or metallic phase.

* Corresponding author.

0022-3115/$ - see front matter © 2004 Elsevier B.V. All rights reserved.
doi:10.1016/j.jnucmat.2004.09.023

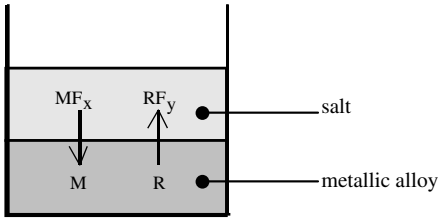

Fig. 1. Sketch of the mass transfer of species by an oxygen–reduction reaction between a metallic alloy and a mixture containing fluorinated salt.

In order to compare results from various experiments, we assume that the concentration $C_j(t)$ of a compound j in the corresponding phase varies with time according to the following relationship:

$$\frac{dC_j}{dt}(t) = k_j \frac{A}{V_j}(C_j^i - C_j(t)), \tag{2}$$

where A, V_j, and C_j^i are respectively the area of the interface, the volume of the phase in which the compound j is present and the concentration of this compound at the interface.

Eq. (2) introduces the capacity time $T_{ca,j}$ characteristic of the transfer of one element j in its phase and is defined as

$$T_{ca,j} = \frac{V_j}{k_j A}. \tag{3}$$

Assuming that the concentration of an element is always equal to its equilibrium concentration, the integration of Eq. (2) leads to the conventional equation:

$$\mathrm{Ln}\left(\frac{C_j - C_j^e}{C_j^0 - C_j^e}\right) = -k_j \frac{A}{V_j} t = -\frac{t}{T_{ca,j}}, \tag{4}$$

where C_j^e is the equilibrium concentration taken as the concentration at the end of the test and C_j^0 is the concentration at the starting time. Within the framework of the film theory, the plot of $\mathrm{Ln}((C(t) - C^e)/(C^0 - C^e))$ versus time must give a line with a slope proportional to the transfer coefficient.

It appears that in the case of the transfer of actinides from a fluoride mixture, characterized by a rather complex transfer mechanism, the variation of the concentration of the species with time is probably not as simple as that which is described by Eq. (2). Nevertheless, the kinetic study presented in this paper will use the concept of capacity time to describe the transfer kinetics of zirconium and uranium (a surrogate of the actinides) from the fluorinated salt towards a metal. Details on the use of Eq. (4) are provided in Appendix A.

When transfer is controlled by the chemical reaction, k_j represents the kinetic constant of the chemical reaction involving species j. This constant is temperature-dependent according to an Arrhenius law. When the transfer is controlled by diffusion, k_j corresponds to the mass-transfer coefficient for species j (often written as h_j).

We investigated the transfer kinetics of the actinides and lanthanides from a fluorinated salt phase into a metal phase including a reducing agent. By monitoring the concentrations in one of the phases during the exchange and interpreting the results based on Eq. (4), we are able to demonstrate that:

- stirring plays an important role,
- material transfer at the interface does not appear to be the only limiting factor.

The latter observation is rare in literature related to this type of process. For instance, some previous studies [5] have shown that the reduction of neptunium by lithium dissolved in liquid bismuth is very long, leading to the assumption that the kinetics are limited by diffusion phenomena.

2. Principle and experimental method

To obtain kinetic data, experiments were performed on two complementary systems. The tests carried out respectively with the first and second systems are summarized in Table 1.

The first system was used to study the kinetics of reduction and transfer for LaF_3, SmF_3, UF_4, ZrF_4, and CrF_3. Each compound was first dissolved at a concentration of 4 mol% in the $LiF–CaF_2$ eutectic at 720 °C.

Table 1
Characteristics of the tests carried out using the two systems

	System 1	System 2
Metal/salt	Zn–Mg/$LiF–CaF_2$	Al–Cu/$LiF–CaF_2–MgF_2$
Transferred element	Sm–La–Zr–Cr–U	Zr
Crucible diameter (mm)	40	90
Stirring technology	Mechanic paddle	Two-frequency magnetic field
Heating technique	Furnace	Induction
Sampling	Metal or salt	Metal

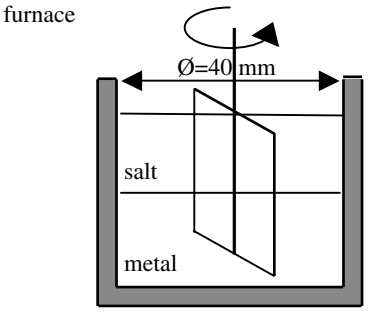

Fig. 2. Sketch of the first experimental system.

Zn–Mg metal alloy containing 1 wt% magnesium was then poured into the molten salt at time $t = 0$. The experimental system was previously described in a thermodynamic study of two-phase equilibrium [2,3] and is sketched in Fig. 2 and summarized in Table 1. It is important to recall that the experimental environment has to be very clean and weak in oxygen in order to avoid the formation of an interfacial layer that could disturb the chemical transfer. The two phases were stirred with a paddle (dimensions: $15 \times 40\,mm^2$) at different rates between 2 rpm and 50 rpm. Samples of a few hundred milligrams of salt were taken at timed intervals by solidification on the cold tip of a stainless steel rod. This rod was very quickly dipped into the melt above the interface and then rapidly removed from the reactor. The stirring is stopped during the sampling that lasts a few seconds. Assuming that no material buildup exists at the interface, the kinetics of removal of the elements from the salt was identical to those of the appearance of the same elements in the metallic phase. The salt samples were then dissolved in perchloric or sulfuric acid for optical ICP analysis.

The second experimental system was used to study the kinetics of reduction and transfer of ZrF_4. It was based on the same chemical principle but with different geometry and type of stirring. The experimental set-up is sketched in Fig. 3 and summarized in Table 1. Heating and stirring were carried out by induction using a two-frequency electric current defined by the following relation:

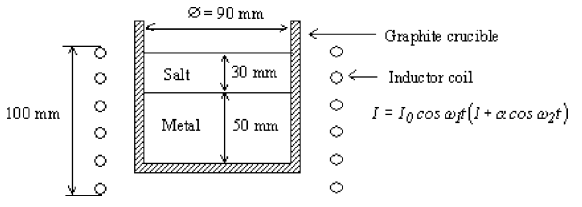

Fig. 3. Experimental device using two-frequency magnetic field for heating and stirring.

$$I = I_0 \cos \omega_1 t(1 + \alpha \cos \omega_2 t), \quad (5)$$

where t is time, ω_1 the high angular frequency needed for heating and bulk stirring and ω_2 the low angular frequency used to agitate the interface. For this purpose, ω_2 must be approximately equal to one of the natural frequencies or half one of the natural frequencies of the interface. The entire experimental system and the stirring method have been described elsewhere [4]. ZrF_4 was dissolved at a concentration of 11 wt% in the eutectic $LiF–CaF_2–MgF_2$. A metal alloy, Al–Cu containing 70 wt% aluminium, was poured into the molten salt at time $t = 0$. In this system, aluminium is used as both a reducing agent and a metal solvent.

Depending on the experiment, the temperature varied between 800 °C and 900 °C. The electromagnetic stirring of the metallic phase produced a velocity of around $2\,cm\,s^{-1}$. Three grams of metallic samples were taken from the bulk at regular intervals. The samples were then dissolved and analysed by optical ICP analysis.

The salts were prepared the same way for both systems. The fluorides were dehydrated in a suitable oven using a fluorinating chemical agent (ammonium difluoride: NH_4FHF). The over-saturated salt + NH_4FHF mixture was introduced into a vitreous carbon crucible and placed in an airtight oven. A 3-h residence time at 180 °C was sufficient to melt the ammonium difluoride and to form complexes with the fluorides to be dehydrated. The water was released as steam and re-condensed in the cold zone. A second treatment for 6 h at 480 °C under flowing argon further modified the complexes, leaving a very dry fluoride. The ammonium fluoride evaporated and re-condensed in the cold zone. After cooling to room temperature, the salt was stored in a dry argon atmosphere in a glove box.

3. Experimental results

3.1. Results without stirring

Initial experiments carried out with both experimental systems and without significant stirring produced a two-phase ingot in which the saline phase contained a black layer as shown in Fig. 4 – left. This phenomenon, already observed by other authors [5] and not clearly explained, is probably related to remote reduction of a species directly in the salt. A chemical investigation carried out by electronic scan microscopy and electronic microsounder (EDS-WSD) does not show significant difference between the composition of the white area and the composition of the black layer, except the presence of pure metallic particles in the black layer as shown in Fig. 10.

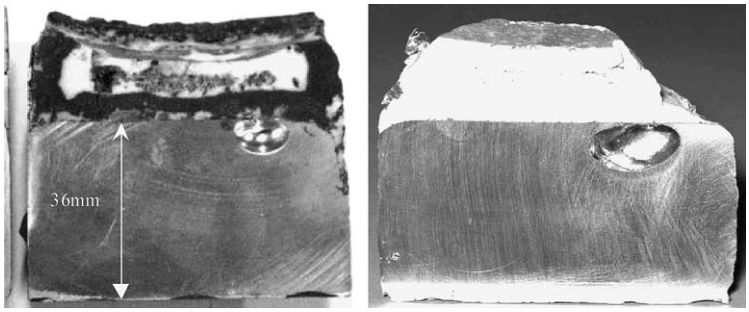

Fig. 4. Qualitative results of equilibrium obtained without agitation or with agitation tangential (left) and with agitation normal to the free surface (right).

3.2. Results with stirring

Three kinds of stirring were used.

(1) In the first experimental system, the entire system is agitated by the paddle, even the interface. The main direction of stirring is tangential to the interface.
(2) For the second experimental system, with a single-frequency induction current, only the bulk of the metallic phase is agitated. Near the interface, the low velocity of around $2\,cm\,s^{-1}$ is mainly tangential to the interface. By continuity of the tangential velocity component, the liquid salt can also be slightly agitated.
(3) For the second experimental system, with a two-frequency induction current, ω_2 being adjusted, both the metallic phase and the interface are agitated. In that case, the main velocity at the interface is normal to the interface.

Quantitative results were obtained for the different types of stirring.

For case 1, the agitation of the whole system leads to the total disappearance of the black layer at the end of the 150 min of testing.

For case 2, the agitation of the metallic phase decreases the thickness of the black layer. In Fig. 5, the measured thickness of this layer is plotted versus the test duration. We note that the thickness of the black layer first increases from 2 to 6 mm and then decreases to 2 mm, never disappearing. The tests never lasted more than 60 min.

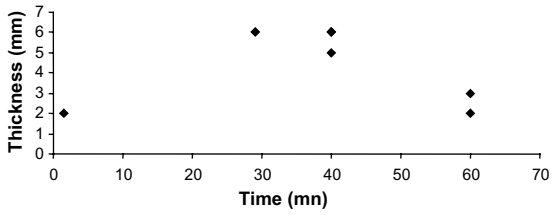

Fig. 5. Evolution of the thickness of the black layer versus time when the metallic phase is agitated only.

For case 3, the agitation of the interface at its natural frequency leads to the total disappearance of the layer as shown in Fig. 4 – right.

The observation of the changes in the black layer lead to the following conclusions. Whatever the type of stirring, the thickness of the black layer decreases. It can even disappear for mixing of sufficient duration or high effectiveness. As soon as the velocity field exhibits a non-zero component normal to the interface, the level of agitation influences the rate of transfer. The kinetics are increased by a factor of 5. This is due to the fact that a fresh mass-transfer interface is generated permanently by this type of agitation which also produces an increase in this surface-area.

Results obtained using system 1 are shown in Fig. 6 for the transfer of uranium (a surrogate for the actinides) and lanthanum (a surrogate for the lanthanides). In both cases, the reducing agent disappears from the salt phase at the same rate as the MgF_2 appears due to oxidation of magnesium. The reduction of lanthanum (normally stable with regard to magnesium) is related to the very strong interactions with the zinc, as its activity coefficients are extremely low (around 10^{-8}) [2]. The reduction of uranium is extremely rapid (just a few minutes) and inconsistent with the several hours generally required for actinide transfer studies under the same conditions [5].

According to Eq. (4), we plot $\mathrm{Ln}((C(t) - C^e)/(C^0 - C^e))$ versus time for each element for the first few minutes (explanations concerning this choice are provided in Appendix A) as shown in Fig. 7. The slope of each straight line (maybe not for chromium) shown in Fig. 7 gives the value of $k_j \cdot (A/V_j)$. The experimental error and the error on the determination of the A/V_j ratio were estimated at 15%; the resulting measurements were therefore assigned an error of about 20%. The

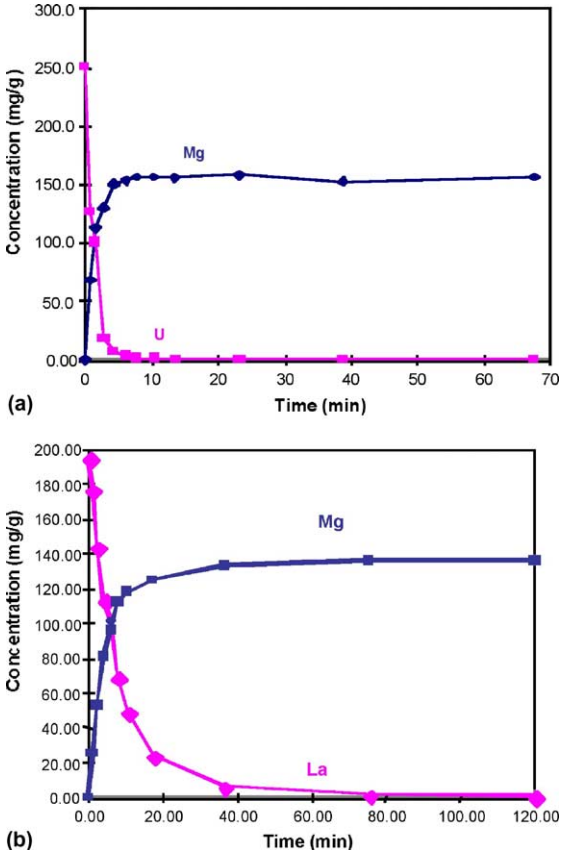

Fig. 6. Mass concentration of the salt phase during transfer of U (a) and La (b) from LiF–CaF_2 toward Zn at 720 °C and 50 rpm – system 1.

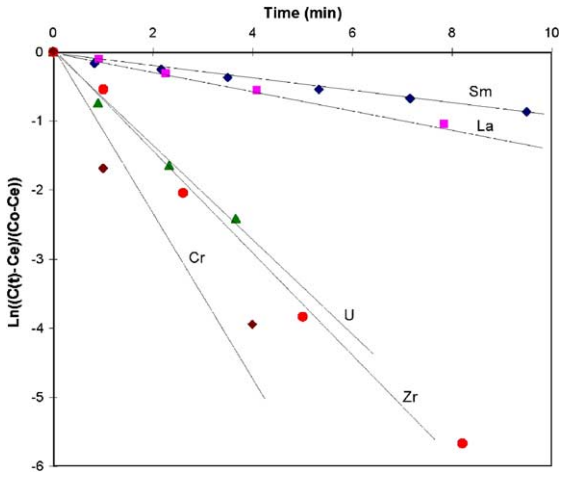

Fig. 7. Graphic plots of $\mathrm{Ln}((C(t)-C^{e})/(C^{0}-C^{e}))$ for various elements from LiF–CaF_2 into Zn–Mg at 720 °C and 50 rpm – system 1.

series of tests conducted at 50 rpm were supplemented by other tests at different stirring speeds. The k_j values measured using this method are shown in Table 2.

These results lead to two conclusions

- The measured k_j values are independent of the stirring speed. This is an unusual result for a pyrochemical process, generally dependent on the hydrodynamic conditions. The transfer kinetics in the test systems thus appears to be controlled by the chemical reaction. k_j will be considered as a kinetic constant related to the temperature by an Arrhenius law (see Section 4).
- The kinetics of Sm and La (surrogates of lanthanides) are lower than the kinetics of Cr, Zr, and U (surrogates of actinides). The value of k_{La} for a stirring rate of 30 rpm is around double than the values obtained for all other stirring rate. We do not have any explanation of this anomaly that can be connected with an error of analysis or an error of sampling. The most important is that the order of magnitude remains stable.

The experiments carried out regarding the transfer of zirconium towards an aluminium copper alloy using electromagnetic stirring (system 2) give complementary results. Table 3 shows the values of k_{Zr} versus different surface agitation rates represented by the values of the surface velocity $\omega_2\eta_0$ where ω_2 and η_0 are respectively the low angular frequency of the electrical induction current and the characteristic height of the fluctuation of the interface. The measurement of the characteristic height was previously described [11] and consists of a pin placed above the surface of the liquid metal. The study of the deformation is made through this pin that is connected to a recording system.

In Table 3, the first two lines correspond to type 2 stirring (cf. Fig. 8). The third line corresponds to a two-frequency type induction current with ω_2 not tuned to the natural or half of the natural frequency of the interface, leading to a small amplitude of the time dependent deformation of the free surface that is difficult to qualify. The remaining three lines corresponds to type 3 stirring.

When only the metallic phase is stirred, the measured value is about $k_{Zr} = 10^{-4}\,\mathrm{m\,s^{-1}}$, highly consistent with the value of k_{Zr} in Table 2.

Considering the four lasted lines of Table 3, also represented in Fig. 8, we see that the mass transfer (including the error on k) increases with the agitation of the interface according to

$$k_{Zr} \propto (\omega_2\eta_0)^{0.3}. \quad (6)$$

Therefore, depending on the way agitation is performed

Table 2
Experimental k_j coefficients ($m\,s^{-1}$) for Sm, La, U, Zr and Cr transfers from $LiF–CaF_2$ into Zn at 720 °C for various stirring rates – system 1

rpm	2	10	30	50
k_{Sm}	$(1.5 \pm 0.3) \times 10^{-5}$	–	–	$(1.4 \pm 0.3) \times 10^{-5}$
k_{La}	$(2.1 \pm 0.4) \times 10^{-5}$	$(2.4 \pm 0.5) \times 10^{-5}$	$(4.7 \pm 0.9) \times 10^{-5}$	$(2.0 \pm 0.4) \times 10^{-5}$
k_U	$(1.0 \pm 0.2) \times 10^{-4}$	$(1.1 \pm 0.2) \times 10^{-4}$	–	$(8.0 \pm 1.6) \times 10^{-5}$
k_{Zr}	–	$(1.1 \pm 0.2) \times 10^{-4}$	–	$(1.0 \pm 0.2) \times 10^{-4}$
k_{Cr}	$(2.1 \pm 0.4) \times 10^{-4}$	–	–	$(2.3 \pm 0.5) \times 10^{-4}$

Table 3
Experimental k_{Zr} coefficient for Zr transfer from $LiF–CaF_2–MgF_2$ into Al–Cu at various surface agitation rates depending on $\omega_2\eta_0$ – system 2

$\omega\eta_0$	T (°C)	k_{Zr} ($m\,s^{-1}$)
$<10^{-2}$	800	$(1.6 \pm 0.2) \times 10^{-4}$
$<10^{-2}$	780	$(1.0 \pm 0.5) \times 10^{-4}$
$\approx 10^{-2}$	807	$(2.5 \pm 1.0) \times 10^{-4}$
0.028	860	$(4.3 \pm 1.3) \times 10^{-4}$
0.150	910	$(7.8 \pm 4.5) \times 10^{-4}$
0.451	855	$(8.1 \pm 3.4) \times 10^{-4}$

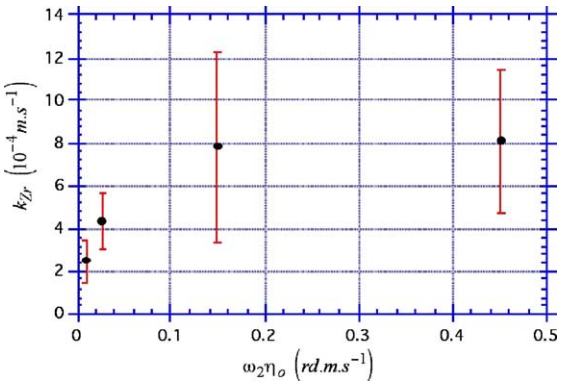

Fig. 8. Evolution of the kinetic of mass transfer of Zr versus the agitation of the free surface.

- the level of bulk agitation has only a slight effect on the rate of transfer when the direction of the velocity near the interface is mainly tangential to this interface,
- the level of the agitation significantly influences the rate of the transfer as soon as the velocity field exhibits a non-zero component normal to the interface.

3.3. Temperature variations

Using system 1, we carried out an experiment to check the variation of the temperature with time. Reduction was achieved according to test 1 (cf. Table 1), using a mixture (representing 40 wt% of the total) of $BaF_2–LaF_3–ZrF_4–CrF_3–ZnF_2$ (5.1–23.8–18.1–2.8–50.2%) dissolved in the $LiF–CaF_2$ solvent (53–47%) with an alloy of Zn containing 4.6 wt% of Mg. The temperature in the furnace and in the system was recorded and is plotted in Fig. 9. Overheating clearly occurs in this system, with the temperature of the crucible reaching 820 °C. This value is in accordance with the discussion presented in Section 4.

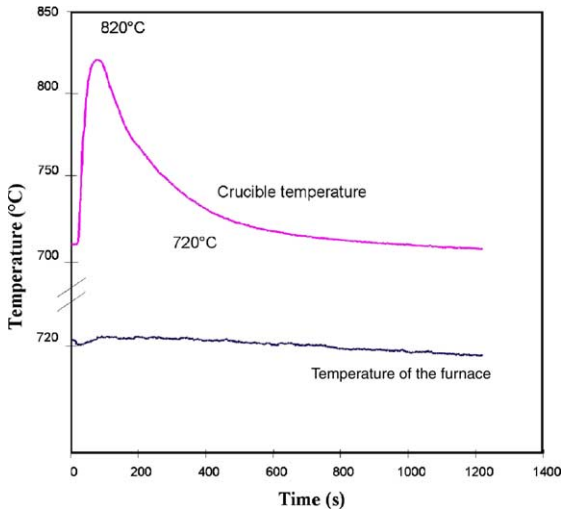

Fig. 9. Recording of the temperature in the furnace and in the crucible during the reduction of a mixture of fluoride by magnesium – system 1.

For system 2, temperature was recorded in all experiments; the maximum measured variation was 20 °C.

These results are not contradictory given that the experiments performed using Al as solvent are much less exothermal than experiments performed using Mg.

4. Discussion

4.1. Black layer and mass-transfer mechanism

For the case without stirring, a black layer appears on the salt side of the system. The appearance of this black layer is always correlated with the existence of pure

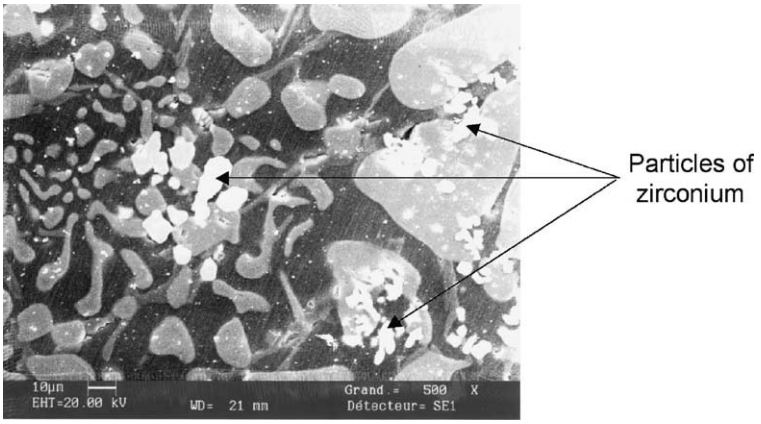

Fig. 10. Particles of pure zirconium in the bulk of the saline phase.

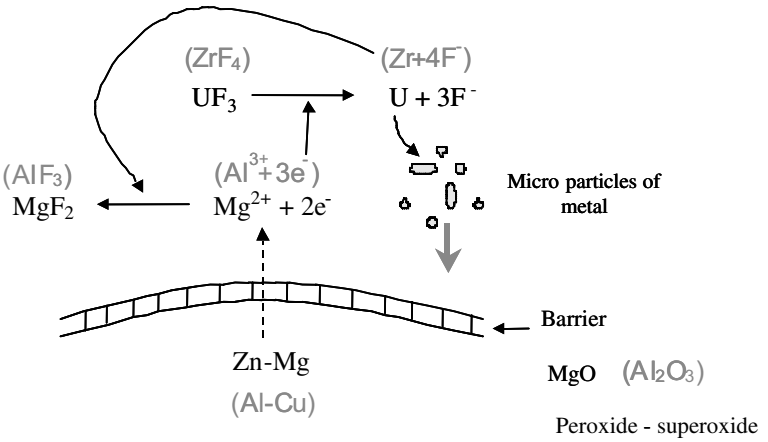

Fig. 11. Mechanism of the reduction through a semi-permeable skin of oxide explaining the presence of pure metallic particles in the saline phase.

metallic precipitates in the saline phase as shown in Fig. 10 where particles of metallic zirconium are seen in the bulk of the saline phase. Similar results are found whatever the element reduced (uranium, chromium, lanthanum, etc.). For cases with stirring, the metallic particles in the saline phase disappear but, as already pointed out, the black layer fully disappears only for long-duration or type 3 stirring. The following mechanism is proposed for the mass transfer of M, as illustrated in Fig. 11.

Because some oxygen remains in the system, a very thin semi-permeable skin of oxide (MgO or Al_2O_3 depending on the reactive system) forms around the metallic phase. This skin could also be made of peroxide and superoxide ions that can aggregate to the interface to form a barrier to the transfer of Mg (or Al). When the system is agitated with a sufficient speed, the barrier is locally broken and the reaction occurs at the interface (this is not the case with a single-frequency induction current that induces a tangential velocity of a few centimetre per second). All the elements that can be reduced are transferred toward the metallic phase. The Mg^{++} ions and two electrons (respectively $Al^{3+} + 3e^{-}$) cross the interface and allow the mechanisms described in Fig. 11 to occur, leading to the precipitation of microparticles of metal (Zr, U, etc.). These particles fall freely in the liquid salt, crossing the interface and generating intermetallic compounds in the metallic phase.

When the system is not agitated, the reaction cannot occur at the interface. In this case either the Mg^{++} ions and two electrons (respectively or the Al^{3+} ions and three electrons) diffuse through barrier as shown in Fig. 11.

4.2. Activation energy

For type 1 or type 2 stirring, the experimental transfer coefficients are given in Tables 2 and 3 and lead to four main conclusions:

- The transfer kinetics are very high for all reduced elements. This is unusual for a pyrochemical process.
- The kinetics depend on the transferred element. For instance, the rate of transfer is higher for uranium (of the order of 10^{-4}) than for lanthanum (of the order of 10^{-5}). These elements can therefore be separated.
- The transfer kinetics are unaffected by the rate of type 1 stirring. This suggests that the limiting factor is the chemical reaction and not mass transfer.
- The transfer kinetics are increased when the interface is agitated with a vertical component (type 3 stirring) and depend on the level of this agitation.

The three first points may be interrelated. Below, we propose an explanation regarding all reactions of reduction by magnesium.

ΔH^0_M and ΔH_s being respectively the quantity of heat exchanged during the reaction and the quantity of heat received by the 'metal + salt' system and assuming an adiabatic heat exchange during the experiment (i.e. $\Delta H^0_M = -\Delta H_s$), we may write:

$$\Delta H^0_M = -nC^s_p \Delta T, \tag{7}$$

where C^s_p, n and T are respectively the apparent molar heat capacity of the overall system, the quantity of solvent material (see Appendix B) and the temperature difference $T_2 - T_1$ between the initial and final states.

Now, considering that the initial $k_{M,1}$ and final $k_{M,2}$ kinetics are related by an Arrhenius law, we may write:

$$k_{M,1} = k_{M,2} \exp\left(\frac{E_{A,M}}{RT_1T_2}(T_2 - T_1)\right), \tag{8}$$

where $E_{A,M}$ and R are respectively the activation energy of the reaction (1) and the perfect gas constant.

Introducing Eq. (7) in Eq. (8) leads to the following relation between the kinetic constants and the reaction enthalpy:

$$k_{M,1} = k_{M,2} \exp\left(-\frac{E_{A,M}}{nC^s_pRT_1T_2}\Delta H^0_M\right). \tag{9}$$

Eq. (7) and the thermodynamic data available in the literature [6–10] can be used to calculate ΔH^0_M for each reaction (see Appendix B). The measured k_M values are plotted against the calculated ΔH^0_M values in Fig. 12. An exponential curve has been fitted to the data. The best-fit curve presents an exponential regression coefficient equal to 0.99.

$$k_M = 3 \times 10^{-5} \exp(-7 \times 10^{-6} \cdot \Delta H^0_M). \tag{10}$$

Theoretical Eq. (9) and experimental Eq. (10) lead to the following values whatever the compound M:

$$k_{M,2} = 3 \times 10^{-5}\,\mathrm{m\,s^{-1}} \quad \text{and} \quad \frac{E_{A,M}}{nC^s_pRT_1T_2} = 7 \times 10^{-6}. \tag{11}$$

Note that k_2 is of the same order of magnitude as the kinetics reported in Tables 2 and 3. Both kinetics k_2 and the activation energy E_A are irrespective of M, indicating that, at any given temperature, the kinetic constants are equivalent regardless of the element reduced and the activation energies are of the same order of magnitude. This may be attributed to the fact that the reaction mechanisms are similar for each reduction process, with the same chemical balance given by Eq. (1) in identical solvents.

Eq. (11) now allows us to calculate E_A considering that

- T_1 corresponds to the temperature at the beginning of the reaction (720 °C).
- T_2 is the temperature rise due to enthalpy transfer (Eq. (7)). It is unknown, but greater than 1000 K and less than 1180 K, the boiling point of zinc. This uncertainty concerning the temperature induces an error in the calculated E_A value.
- The molar heat capacities of the phases are available in the literature [12] (see Appendix B) and are used to determine the mean heat capacity of the metal-salt systems used, which contain 1 mol of LiF, 0.2 mol of CaF_2 and 1.2 mol of Zn. Therefore

$$n \cdot C_p \approx 115\,\mathrm{J\,K^{-1}}.$$

- n_{Mg} is the number of moles of the reduced species and the quantity of material reduced during each experiment was $n_{Mg} = 4 \times 10^{-2}$ mol.

E_A is then expressed as follows:

$$E_A = 7 \times 10^{-6} \frac{nC^s_pRT_{ini}T_{fin}}{n_{Mg}}, \tag{12}$$

$$E_A = 182 \pm 15\ \mathrm{kJ\,mol^{-1}}.$$

The value is too high for to be the activation energy of diffusion-limited kinetics, but presents the right order

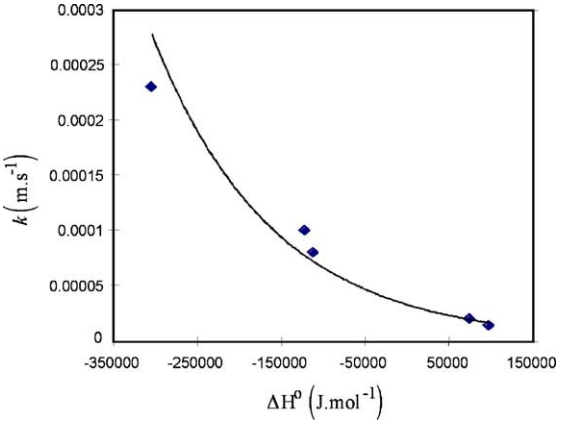

Fig. 12. k versus ΔH^0 for k_i measured at 720 °C and 50 rpm.

of magnitude for transfer kinetics limited by the chemical reaction. This is consistent with the results observed for stirring, i.e. no effect on the kinetics but an effect on the dissipation of heat produced by the chemical reaction corresponding to the mechanisms described above.

5. Conclusion

The kinetics of the transfer of various elements between a fluorinated salt phase and a liquid metal phase mixture have been studied using two complementary experimental systems. Different kinds of stirring were tested.

In the absence of stirring, no transfer takes place. The reason may be related to the existence of an oxide layer at the interface. With stirring, the layer disappears and the transfer takes place. It has been shown that the kinetics is increased when the interface is agitated with a vertical component of the velocity and depends on the level of this agitation. Furthermore, a black layer containing pure particle of metal is observed in the saline phase with a weak stirring. Two types of explanations are proposed to understand our results: the first involves the hydrodynamics of the baths and the second the thermochemistry of the system.

Depending on the way agitation is performed, the stirring rate affects or does not affect the kinetics. When the velocity near the interface is mainly tangential to the interface, the level of agitation is sufficient to break oxide layer, but has only a limited effect on the rate of transfer. As soon as the velocity field increased and includes a non-zero component normal to the interface, the level of agitation increases the mass-transferring surface and influences the kinetics.

A simple model based on first-order kinetics provides a relation between the kinetic constants and the reduction enthalpy values. The resulting law is fully validated by our experimental findings and has been used to determine a reaction activation energy of about $182\,\mathrm{kJ\,mol^{-1}}$. This very high value probably corresponds to kinetics limited by the chemical reaction what is rather unusual for a pyrochemical process, suggesting a relatively complex reaction mechanism that will require more thorough analysis.

Indeed, this study has shown that in two-phase liquid systems, some elements such as uranium and zirconium are reduced directly in the salt, forming metal precipitates in the salt phase and suggesting possible electron transfers from the metal phase into the salt phase. More work is required to better understand the reaction mechanism and determine how the black layer is formed and what can be its influence on the separation process.

Acknowledgment

The authors are grateful to the referee whose remarks allowed improvements in the presentation of their results.

Appendix A. Analysis of the data

To compare different experimental results, we use the following equation:

$$\mathrm{Ln}\left(\frac{C_j - C_j^{\mathrm{e}}}{C_j^0 - C_j^{\mathrm{e}}}\right) = -k_j \frac{A}{V_j} t = -\frac{t}{T_{\mathrm{ca},j}}. \tag{A.1}$$

Fig. A.1 shows a typical plot of the concentration of zirconium in the metal in system 2 versus time. After a certain time, the Zr-composition reaches $C_{\mathrm{Zr}}^{\mathrm{end}}$ which is close to the expected final value. The curve $\mathrm{Ln}((C_{\mathrm{Zr}}(t) - C_{\mathrm{Zr}}^{\mathrm{end}})/C_{\mathrm{Zr}}^{\mathrm{end}})$ plotted over the full duration of the test (Fig. A.2) shows a linear zone in the first few minutes (maybe not for the chromium), followed by a significant deviation from this line. This can be attributed to the increasing error in slope as the concentrations approach equilibrium. The slope of the linear regression of the first points gives the kinetics of the mass transfer for the experiment.

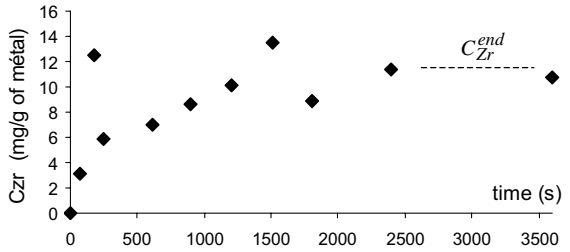

Fig. A.1. Mass concentration of zirconium in the metal versus the time. Experiments are performed in system 2 at 850 °C without modulation. The typical magnetic field is 7.8 mT.

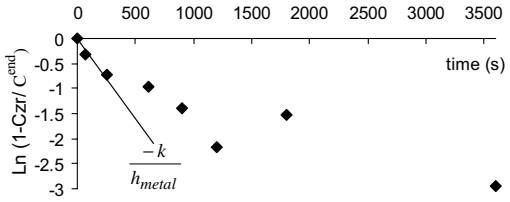

Fig. A.2. Graphic plots of $\mathrm{Ln}((C_{\mathrm{Zr}}(t) - C_{\mathrm{Zr}}^{\mathrm{end}})/C_{\mathrm{Zr}}^{\mathrm{end}})$. Mass concentrations of zirconium in the metal correspond to Fig. A.1.

Table B.1
Standard enthalpy of formation of compound i

Compound i	MgF_2 [7]	AlF_3 [7]	CrF_3 [6]	ZrF_4 [7]	UF_4 [8]	LaF_3 [10]	SmF_3 [10]
$\Delta_f H_i^0$ (kJ mol^{-1})	−1083	−1506	−1168	−1911	−1897	−1698	−1633

If the second term of Eq. (A.1) is designated by a, the uncertainty (δa) is then:

$$\delta a = \frac{1}{C^0 - C^e}\left[\delta C^0 - \delta C^e - \frac{C^0 - C^e}{C(t) - C^e}(\delta C(t) - \delta C^e)\right]. \tag{A.2}$$

For both systems, $C^0 \gg C^e$ in the salty phase. Assuming that $\delta C^0 \gg \delta C^e$, the error on k can be estimated over short and long periods: short periods

$$C(t) \approx C^0 \quad \text{and} \quad \frac{\delta a}{a} \approx \frac{\delta C^0}{C^0}\left(\frac{1 - e^a}{a}\right) \approx \frac{\delta C^0}{C^0},$$

long periods

$$C(t) \approx C^e \quad \text{and} \quad \frac{\delta a}{a} \approx \frac{1}{C^0}\left(\frac{\delta C^0}{a} - \frac{2e^a \delta C^e}{a}\right) \to \infty.$$

The uncertainty in C^0 is about 5% and therefore the error in k is initially of the same order of magnitude. For this reason, we limited the interpretation of the graphs to the first few minutes of each test. Beyond this duration, the uncertainty tends toward infinity and the graphs no longer provide meaningful information.

Appendix B. Determination of ΔH_M^0 and C_p^s

We will now calculate the quantity of heat exchanged ΔH_M^0 during reduction by reducing agent R (magnesium or aluminium) and the molar heat capacity C_p^s of the overall system.

Consider reduction by reducing agent R for one mole of F_2 exchanged

$$\frac{2}{x}MF_x + \frac{2}{y}R \leftrightarrow \frac{2}{y}RF_y + \frac{2}{x}M. \tag{B.1}$$

We may write:

$$\Delta H_M^0 = \frac{2}{y}\Delta_f H^0_{RF_y} - \frac{2}{x}\Delta_f H^0_{MF_x}, \tag{B.2}$$

where $\Delta_f H_i^0$ is the standard enthalpy of formation of compound i, available in the literature [6–10] and given in Table B.1.

The molar heat capacity C_p^s of the overall system is expressed as follows:

$$C_p^s = \sum n_i C_p(i), \tag{B.3}$$

Table B.2
Number of moles and molar heat capacity of solvent compound i

Solvent compound i	LiF	CaF_2	Zn
n_i (mol^{-1})	1.0	0.2	1.2
$C_p(i)$ (J mol^{-1} K^{-1})	59.6	90.1	31.4

where n_i is the number of moles of the solvent compound i and $C_p(i)$ is the molar heat capacity of the solvent compound i, available in the literature [6–10] and given in Table B.2.

References

[1] F.D. Richardson, Physical Chemistry of Melts in Metallurgy, vol. 2, Academic Press, London, 1974.
[2] F. Lemort, X. Deschanel, R. Boen, M. Allibert, Global '99, August 29th–September 3rd, Jackson Hole, Wyoming, USA.
[3] F. Lemort, X. Deschanel, R. Boen, L. Rault, M. Heusch, M. Allibert, Nucl. Technol. 139 (2) (2002) 167.
[4] D. Perrier, Y. Fautrelle, J. Etay, F. Lemort, R. Boen, in: 5th International Conference on 'Fundamental and applied MHD' 2002, 16–20 September, Ramatuelle, France.
[5] H. Moriyama, M. Miyazaki, Y. Asaoka, K. Moritani, J. Oishi, J. Nucl. Mater. 182 (1991) 113.
[6] I. Barin, O. Knacke, O. Kubaschewski, Thermodynamic Properties of Inorganic Substances, Springer, Berlin, 1973, Suppl. 1977.
[7] I. Barin, Thermochemical Data of Pure Substances, VCH Verlags Gesellshaft, Weinheim, 1993.
[8] I. Barin, Thermochemical Data of Pure Substances, VCH Verlags Gesellshaft, Weinheim, 1989.
[9] L.P. Ruzinov, B.S. Guljanickij, Ravnovesnye prevrasoenijametallugiceskin reaktseij, Moskva, 1975.
[10] O. Knacke, O. Kubaschewski, K. Hesselmann, Thermochemical Properties of Inorganic Substances, Springer, Berlin, 1991.
[11] D. Perrier, Y. Fautrelle, J. Etay, Experimental and theoretical studies of the motion generated by a two-frequency magnetic field at the free surface of a gallium pool, Met. Trans. B (2002).
[12] Smithells, Données Thermophysiques des métaux, 7th Ed., Ed. E.A. Brandes and G.B. Brook.